

Article

Interaction of Freshwater Diatom with Gold Nanoparticles: Adsorption, Assimilation, and Stabilization by Cell Exometabolites

Aridane G. González ^{1,2}, Oleg S. Pokrovsky ^{2,3,*} , Irina S. Ivanova ^{4,5} , Olga Oleinikova ², Agnes Feurtet-Mazel ⁶, Stephane Mornet ⁷ and Magalie Baudrimont ⁶

¹ Instituto de Oceanografía y Cambio Global, IOCAG, Universidad de Las Palmas de Gran Canaria (ULPGC), 35001 Las Palmas, Spain; aridaneglez@gmail.com

² Géosciences Environnement Toulouse (GET), UMR 5563, CNRS-OMP-Université Toulouse, 14 Avenue Edouard Belin, 31400 Toulouse, France; olga-oleyn@yandex.ru

³ BIO-GEO-CLIM Laboratory, Tomsk State University, Lenina 36, 634050 Tomsk, Russia

⁴ N. Laverov Federal Center for Integrated Arctic Research, Russian Academy of Science, 119991 Arkhangelsk, Russia; ivanovais_1986@mail.ru

⁵ Tomsk branch of the Trofimuk Institute of Petroleum Geology and Geophysics, SB RAS, Tomsk, Akademichesky 4, 634055 Tomsk, Russia

⁶ UMR Environnements et Paléoenvironnements Océaniques et Continentaux (EPOC) 5805, Aquatic Ecotoxicology, Université de Bordeaux, Place du Dr Peyneau, 33120 Arcachon, France; agnes.feurtet-mazel@u-bordeaux.fr (A.F.-M.); magalie.baudrimont@u-bordeaux.fr (M.B.)

⁷ Institut de Chimie de la Matière Condensée de Bordeaux-UMR 5026 CNRS, 33600 Pessac, France; mornet@icmcb-bordeaux.cnrs.fr

* Correspondence: oleg.pokrovsky@get.omp.eu; Tel.: +33-5-61-33-26-25

Received: 22 January 2018; Accepted: 1 March 2018; Published: 5 March 2018

Abstract: The rising concern about the potential toxicity of synthetic gold nanoparticles (*AuNPs*) in aquatic environments requires a rigorous estimation of physico-chemical parameters of reactions between *AuNPs* and major freshwater microorganisms. This study addresses the interaction of 10-nm size, positively charged *AuNPs* with periphytic freshwater diatoms (*Eolimna minima*). The adsorption experiments on viable cells were performed in 10 mM NaCl and 5 mM NaCl + 5 mM NaHCO₃ solution at a variable pH (3–10), at an *AuNPs* concentration from 1 µg/L to 10,000 µg/L, and an exposure time from a few minutes to 55 days. Three types of experiments, adsorption as a function of time (kinetics), pH-dependent adsorption edge, and constant-pH “Langmuirian” type isotherms, were conducted. In addition, long-term interactions (days to weeks) of live diatoms (under light and in the darkness) were performed. The adsorption was maximal at a pH from 3 to 6 and sizably decreased at a pH of 6 to 10. Results of adsorption experiments were modeled using a second order kinetic model, a Linear Programming Model, Freundlich isotherm, and a ligand binding equation for one site competition. The adsorption of *AuNPs*(+) most likely occurred on negatively-charged surface sites of diatom cell walls such as carboxylates or phosphorylates, similar to previously studied metal cations. Under light exposure, the *AuNPs* were stabilized in aqueous solution in the presence of live cells, probably due to the production of exometabolites by diatoms. The adsorbed amount of *AuNPs* decreased after several days of reaction, suggesting some *AuNPs* desorption. In the darkness, the adsorption and assimilation were stronger than under light. Overall, the behavior of positively charged *AuNPs* at the diatom–aqueous solution interface is similar to that of metal cations, but the affinity of aqueous *AuNPs* to cell exometabolites is higher, which leads to the stabilization of nanoparticles in solution in the presence of diatoms and their exudates. During photosynthetic activity and the pH rising above 9 in the vicinity of diatom cells, the adsorption of *AuNPs* strongly decreases, which indicates a decreasing potential toxicity of *AuNPs* for photosynthesizing cells. The present study demonstrates the efficiency of a thermodynamic and kinetic approach for understanding gold nanoparticles interaction with aquatic freshwater periphytic microorganisms.

Keywords: *AuNPs*; freshwater diatoms; biofilm; adsorption; river; pollution

1. Introduction

The rapid growth of the nanotechnology industry has led to the wide-scale production and application of engineered nanoparticles (NP). They are increasingly used in industry, medicine, and various consumer products such as cosmetics, sunscreens, textiles, and food [1], and are therefore released into the environment with domestic sewage. Among different NP materials, gold is widely used at both an industrial level and in biology. For example, gold nanoparticles have been used for the development of real-time optical diagnoses, label-free detection, cellular tracking, tumor treatment, or drug delivery [2,3]. As a result, gold nanoparticles (*AuNPs*) are progressively released in the air and water via erosion, watershed, and industrial or hospital wastes, and these rejects progressively increase each year [4,5]. Together with other nanoparticles in aquatic systems, *AuNPs* are also investigated for their use as decontamination devices. For example, coagulation or flocculation techniques of nanoparticles by organic molecules have been developed [6–8], and the efficiency of gold nanoparticles as low-molecular-weight-chelators in aqueous suspensions has been demonstrated [9]. However, their harmless nature has yet to be proven for living organisms in the natural environment. Different research groups have shown that *AuNPs* exert moderate toxic effects on eukaryotic cells, on animal models, and several organisms representing different levels of ecosystems [10], although these toxic effects greatly depend on particle size and surface coating. It is known that these particles, and in particular amine coated gold nanoparticles, are able to penetrate a high variety of cells [11,12], and are recognized to be highly stable in aqueous solution [5]. At the moment, the impact of *AuNPs* towards aquatic organisms in terms of toxicity and trophic transfer [13] is poorly characterized. Thus, despite their a priori inert character, several studies have already highlighted their toxic properties and notably their capability to generate oxidative stress [10,13–18]. In order to understand the impact of *AuNPs* on freshwater microbial ecosystems, the adsorption of *AuNPs* on cell surfaces should be studied as the first step before *AuNPs* internalization.

Gold nanoparticles pollution in freshwater environments is an issue of rising concern [19,20]. The emergency of European river pollution by industrially produced and domestically and commercially used *AuNPs* calls for a need to rationalize the interaction of these new potentially toxic substances with dominant microorganisms of freshwater ecosystems, such as periphytic diatoms. Adsorption and assimilation of metals, and by analogy, of nanoparticles by aquatic microorganisms, are considered as one of the major process controlling the fate of micro pollutants in the environment. It is known that the first step in a toxicant uptake by biota is the adsorption of NPs on external layers of the cell wall. Thus, numerous studies have been devoted to the quantification and thermodynamic modeling of reversible metal cation adsorption on the cell wall of aquatic microorganisms [21–24]. Extensive research over past decades has provided a comprehensive picture of metal binding to cell walls of most model aquatic microorganisms, including autotrophic and heterotrophic bacteria and diatoms [25–33]. However, there is no study, to our knowledge, of *AuNPs* interaction with freshwater periphytic diatoms.

Therefore, the first goal of the present work was to quantify the stability of *AuNPs* in solution and characterize the adsorption capacities of freshwater diatoms with respect to *AuNPs* under controlled laboratory conditions. In order to model the adsorption equilibria, performing both pH-dependent adsorption edge and metal-dependent (constant-pH) adsorption experiments is crucial for the robustness of the metal adsorption model, because only by independently varying both pH and metal concentration can one rigorously constrain the number and chemical nature of sites involved in metal binding under variable environmental conditions. The second goal of this study was to characterize the long-term (days to weeks) interaction of *AuNPs* with live diatom cells to assess the effect of prolonged exposure of diatoms to nanopollutants. Overall, this study should allow a

physico-chemical level understanding of basic environmental processes which control the uptake of the NP pollutant by diatoms and thus contribute to the development of reliable predictive models describing the impact of nanopollutants on aquatic ecosystems.

2. Materials and Methods

2.1. Diatom Cultures

Monospecific diatom cultures were developed from laboratory strains to produce a biomass of freshwater periphytic *Eolimna minima* (EOMI), as described previously [31,34–37]. Diatoms were cultured to a concentration of $\sim 10^7$ cell/L at 20 °C in a sterile Dauta freshwater medium [38] at pH ~ 7.7 – 7.8 . Before the adsorption experiments, diatoms were rinsed three times in 0.01 M NaCl electrolyte solution using centrifugation at $2200 \times g$ (~ 400 mL of solution for 1 g of wet biomass). The biomass of the diatoms was quantified by its wet (centrifuged 15 min at $4500 \times g$) and dry (lyophilized or freeze dried) weight. Before the adsorption experiment, biomass was removed from the support and rinsed three times in appropriate electrolyte solution using centrifugation at $4500 \times g$ (~ 500 mL of solution for 1 g of wet biomass) to remove, as possible, the adsorbed ions and organic cell exudates from the surface.

2.2. AuNPs Synthesis and Characterization

AuNPs were synthesized following the procedure of Baudrimont et al. [14] to produce spherical and monodispersed nanoparticles. Surfaces were functionalized with heterobifunctional poly(ethylene oxide) macromolecules bearing a thiol group (-SH) in position ω , and a primary amino group (-NH₂) in position α . The thiol groups enable the anchoring of the macromolecule to Au surface sites, while amino groups provide the cationic character of the nanoparticle surface in acid and neutral media. The grafting density was 3.33 molecules/nm², corresponding to 1 mg of functionalized AuNP to a mass of 5.48 μ g of S. A nanoparticle stock solution of a 10.0 ± 0.5 nm average diameter, determined by transmission electron microscopy, and 3.34×10^{17} AuNP⁺/L equivalent to 3.264 g/L concentration, was diluted to various degrees for diatom adsorption and assimilation experiments.

2.3. Short Term AuNPs Adsorption

In order to provide a quantitative description of AuNPs binding onto diatom surfaces, two types of adsorption experiments were conducted: (i) adsorption at a constant initial metal concentration as a function of pH (pH-dependent adsorption edge); and (ii) adsorption at a constant pH as a function of metal concentration in solution (Langmuirian-like isotherm). In order to assess the environmental parameters controlling the interaction of AuNPs with diatom surfaces, effects of biomass concentration and light exposure were also investigated. Adsorption experiments were conducted at 25 ± 0.5 °C in a continuously agitated diatom suspension of 0.01 M NaCl solution or 0.005 M NaCl + 0.005 M NaHCO₃ using 30 mL sterile Teflon (PTFE) containers. All manipulations were conducted in the laminar hood box. The pH-dependent adsorption edges were measured after 2 h of exposure in the dark in order to prevent cell growth and metabolic activity. The pH was adjusted using either NaOH or HCl. Sodium bicarbonate buffer was added to a concentration of 0.005 M in order to keep the pH constant during Langmuirian adsorption isotherm measurements. For all experiments, sterile de-ionized water (Milli-Q, 18.3 M Ω) purged of CO₂ by N₂ bubbling was used. At the end of the experiment, the suspension was centrifuged and the resulting supernatant filtered through a 0.22 μ m Nylon filter, acidified with ultrapure bi-distilled HCl, and stored in the refrigerator before the analysis. The concentration of AuNPs adsorbed on diatoms was calculated by subtracting the concentration of AuNPs in the supernatant from the original amount of metal added in the solution. To account for AuNPs adsorption on the reactor's walls, supernatants obtained from diatom suspensions were conditioned at $3 \leq \text{pH} \leq 9$ and the same concentration of added AuNPs as in cell adsorption experiments. After 2 h, no significant decrease of initial Au concentration was detected upon filtration, indicating the absence of AuNPs adsorption on

the reactor walls and Au hydroxide formation in solutions. Only at $\text{pH} > 6$ and $[\text{AuNPs}]_t > 100 \mu\text{g/L}$ was a $\sim 30\%$ decrease of *AuNPs* concentration in blank experiments observed. This was taken into account when calculating the net adsorption yield.

The adsorption of *AuNPs* on EOMI diatoms was studied as a function of time (0–3 h and 1–55 days), pH (3–10), and *AuNPs* concentration in solution (1–1000 $\mu\text{g/L}$). Although this range of concentration exceeded that of real cases found in contaminated environments linked to industrial and hospital waste, the concentration of diatoms used in our experiments was also several orders of magnitude higher than that encountered in freshwater aquatic environments, so that the ligand to metal ratio in the experiments was similar to that in natural settings. For all of these studies, the cell supernatant obtained after three rinses of cells in the experimental electrolyte solution was considered as a blank. The biomass was kept constant at 0.2 or 0.5 $\text{g}_{\text{wet}}/\text{L}$. The experiments were carried out under permanent stirring and in the darkness at $25 \pm 1 \text{ }^\circ\text{C}$. The contact time was 60 min for pH-edge and langmuirian experiments. In addition, langmuirian adsorption experiments were conducted at a variable initial concentration of *AuNPs* (1–700 $\mu\text{g/L}$) over 1 and 24 h of exposure time. All these experiments were carried out in duplicate.

2.4. Long Term AuNPs Assimilation

Long-term interaction of *AuNPs* with live diatom cells, also run in duplicates, was studied during one to 55 days of reaction, at 20 $\mu\text{g/L}$ of added *AuNPs*, 1 and 10 $\text{g}_{\text{wet}}/\text{L}$ of biomass, and a pH of 8.6 ± 0.3 maintained by a mixture of 0.005 M NaCl + 0.005 M NaHCO_3 . Another series of experiments were conducted under light and in the darkness, over 20 days of exposure, and an initial concentration of added *AuNPs* of 100 $\mu\text{g/L}$. For this, semi-transparent Teflon bottles with *AuNPs*-bearing solution and diatom cells were gently agitated on a ping-pong shaker at $22 \pm 1 \text{ }^\circ\text{C}$. The bottles were aerated using Biosilico porous caps. Over long-term exposure of diatoms to *AuNPs*, an optical microscope examination of cells at the end of experiment demonstrated that the cells remained intact and undeformed, with chloroplasts well-preserved, and some cells were in a state of division.

2.5. Analyses

All filtered solutions were analyzed for Au using graphite furnace atomic absorption (Perkin Elmer AAnalyst 600 spectrophotometer, Perkin Elmer, Waltham, MA, USA) with an uncertainty of $\pm 5\%$ and a detection limit of 0.1 $\mu\text{g Au/L}$. For Au concentrations lower than 1 $\mu\text{g/L}$, analyses were performed by Quadrupole ICPMS-Agilent 7500ce (Agilent, Santa Clara, CA, USA) with an uncertainty of 5% and a detection limit of 0.01 $\mu\text{g/L}$. Values of pH were measured using a Mettler Toledo® (Mettler, Greifensee, Switzerland) combined electrode, with an accuracy of ± 0.01 pH unit. Dissolved Organic Carbon (DOC) was analyzed using a Carbon Total Analyzer (Shimadzu TOC-6000, Shimadzu, Nakagyo-ku, Japan) with an uncertainty of 3% and a detection limit of 0.1 mg/L .

2.6. Modeling

In agreement with available surface titration and spectroscopic data on peryphytic diatoms [26,27,30], we hypothesized that the major metal- and proton-active sites on the diatom cell surface are carboxyl, phosphoryl, phosphodiester, and amine moieties. In order to assess the metal binding strength and capacity of the biofilm surface functional groups, pH-dependent adsorption edge and constant-pH adsorption edge data were modeled using several adsorption models such as the ligand binding equation for a single site competition (pH-dependent), a Linear Programming Model approach (LPM), and Freundlich isotherm for constant-pH adsorption, as presented previously by Martinez et al. [27] and recently applied for modeling the metal cations binding to cyanobacteria [39], phototrophic bacteria [40], soil bacteria [41], and diatom [42] surfaces. To model the pH-dependence of *AuNPs* adsorption, a ligand binding equation for a single site competition was applied (Equation (1)):

$$y = \min + \frac{(max - \min)}{(1 + 10^{pH - \log EC50})} \quad (1)$$

where y is the adsorbed $AuNPs$; \min represents the non-specific binding sites with the same concentrations of y ; \max represents the maximum binding sites with the same concentration of y ; and $\log EC50$ is the pH at which 50% of $AuNPs$ were adsorbed.

The constant-pH adsorption experiments were fitted to an LPM model. Here, the linear programming regression techniques automatically minimize the number of binding sites and the absolute error, $e = [AuNPsB^+]_{T,calc,i} - [AuNPsB^+]_{T,i}$, rather than the least squares. This approach finds one global minimum for the error function, which emphasizes zero as a possible solution and avoids convergence problems such as those found in FITEQL where the solution could be a local minimum [26]. Therefore, the adsorption equation can be considered as Equation (2):



where, B_j represents a specific surface functional group and $K_{m,j}$ the apparent metal-ligand binding constant conditional on ionic strength. For a j -th deprotonated functional group at a fixed pH value, $K_{m,j}$ can be defined as:

$$K_{m,j} = \frac{[AuNPsB_j^+]_i}{[AuNPs^+]_{meas,i} [B_j^-]_i} \quad (3)$$

where $i = 1 \dots n$ represents ligand additions and $j = 1 \dots m$ indicates binding sites. In the above expression, $K_{m,j}$ is a function of experimentally determined metal concentrations, $([AuNPs^+]_{meas,i})$ and of the amount of $AuNPs^+$ bound to the j -th site as a function of increasing biomass and at a fixed pH value, $[AuNPsB_j^+]_i$.

In addition, the constant-pH adsorption was also modeled by using the Freundlich isotherm described by Equation (4):

$$\log[AuNPs]_{adsorbed} = \log k_F + \left(\frac{1}{n}\right) \log[AuNPs]_{solution} \quad (4)$$

where k_F and n are the characteristics parameters of the adsorption reaction on the diatoms.

3. Results

3.1. Short-Term Kinetics of Adsorption

The kinetic experiments were carried out in the presence of 0.2 and 0.5 g_{wet}/L diatoms at a constant pH of 6.4 ± 0.1 and low (4–9 $\mu\text{g/L}$; Figure 1A) and high (111–115 $\mu\text{g/L}$; Figure 1B) initial $AuNPs$ concentrations. These results demonstrated that the adsorption of $AuNPs$ was higher when the higher biomass was used. Note that at a high initial $AuNPs$ concentration, there was no significant difference between the two initial diatom biomasses. It can be seen that 85% of the total amount is adsorbed during the first 100 min of the reaction.

The results were fitted to a second order rate equation (Equations (5) and (6)):

$$\frac{d[AuNPs]}{dt} = -k[AuNPs]^2 \quad (5)$$

$$\frac{1}{[AuNPs]} = \frac{1}{[AuNPs]_0} + kt \quad (6)$$

The half-life time of adsorbed $AuNPs$ is defined by Equation (7):

$$t_{1/2} = \frac{1}{k[AuNPs]_0} \quad (7)$$

The second order rate constants in 0.01 M NaNO₃ and the half-life times of AuNPs in the presence of diatom at two different biomasses are listed in Table 1.

Table 1. Parameters of second order rate equation (Equation (6)) of AuNPs adsorption onto EOMI.

Experiment	Initial AuNPs ($\mu\text{g}\cdot\text{L}^{-1}$)	k ($\text{L}\cdot\mu\text{g}^{-1}\cdot\text{min}^{-1}$)	$t_{1/2}$ (min)
low AuNPs and 0.2 g _{wet} /L EOMI	3.60	7.50×10^{-3}	37.0
low AuNPs and 0.5 g _{wet} /L EOMI	8.50	1.05×10^{-2}	11.2
high AuNPs and 0.2 g _{wet} /L EOMI	115	4.00×10^{-4}	21.8
high AuNPs and 0.5 g _{wet} /L EOMI	111	4.00×10^{-4}	22.5

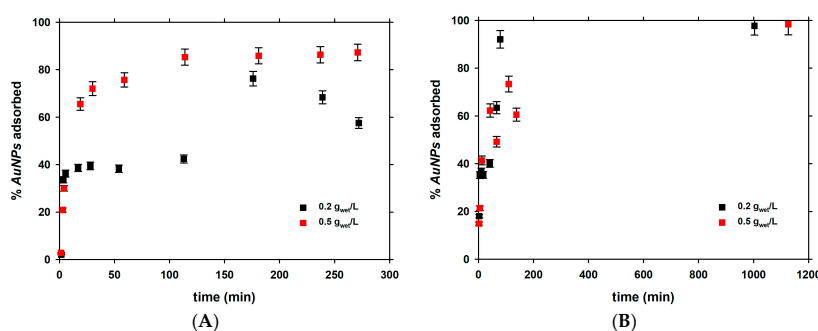


Figure 1. Short-term adsorption kinetics of AuNPs onto 0.2 and 0.5 g_{wet}/L of diatoms EOMI, at two initial AuNPs concentrations (3.6–8.5 $\mu\text{g AuNPs/L}$ (A) and 111–115 $\mu\text{g AuNPs/L}$ (B)) under darkness at pH of 6.4 ± 0.1 . The error bars are within the symbol size unless shown. They correspond to standard deviation of duplicates.

3.2. Dependence of Adsorption of pH

The stability of AuNPs was studied as a function of pH (2.1–12) in 0.01 M NaCl and supernatant produced after rinsing the diatom suspension three times, which was in contact with 0.01 M NaCl for 60 min (Figure 2). The presence of dissolved organic matter (DOM) at concentrations of 0.4 to 0.6 mg DOC/L in solution stabilized AuNPs in solution in the whole range of studied pH (Figure 2), as it has also been demonstrated in laboratory experiments [43,44]. The concentration of AuNPs was three times lower in 0.01 M NaCl compared to that in the supernatant of diatom cultures. The concentration of AuNPs decreased by ca. 15 $\mu\text{g/L}$ at pH from 3 to 12, but decreased three-fold and then remained relatively constant or increased in the NaCl electrolyte.

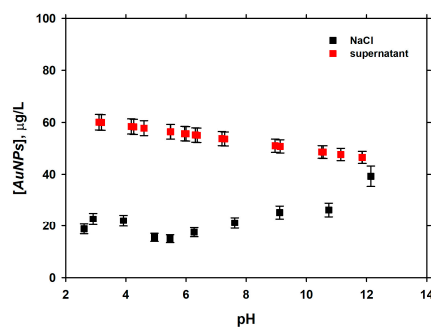


Figure 2. The concentration of AuNPs measured after 60 min in 0.01 M NaCl and in diatom supernatant obtained after reaction with 0.5 g_{wet}/L of biomass. The initial concentration of AuNPs in both cases was 60 $\mu\text{g/L}$. The error bars are within the symbol size unless shown. They correspond to standard deviation of duplicates.

A plot of the percentage of adsorbed *AuNPs* as a function of pH demonstrated that the adsorption of *AuNPs* decreased with an increase in pH, which was especially visible at a pH of 6 to 12 (Figure 3).

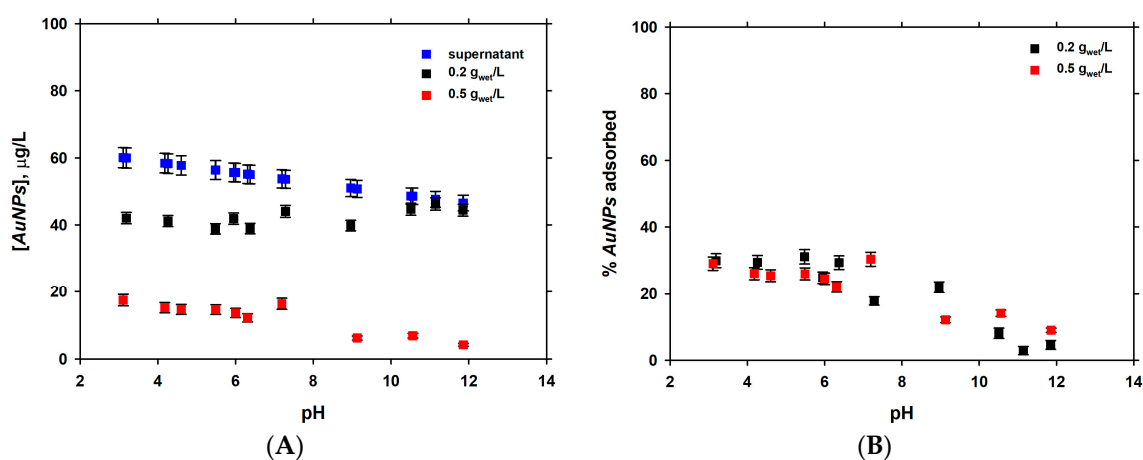


Figure 3. (A) The final concentration of *AuNPs* measured after 60 min in cell-free supernatant and in contact with 0.2 and 0.5 g_{wet}/L of diatoms; and (B) the percentage of adsorbed *AuNPs* as a function of pH. The error bars are within the symbol size unless shown. They correspond to standard deviation of duplicates.

Net adsorption of *AuNPs* at the diatom surface is due to competition with H⁺ for negatively-charged anionic surface sites (phosphorylates, sulphides), as it is fairly well established for divalent metals interacting with diatoms [31,34] and various bacteria [45]. The desorption with the increase of pH may be due to competition between aqueous ligands complexing *AuNPs*⁺ particles and surface site moieties.

The hypothesized complexation between *AuNPs* and aqueous organic ligands at a pH above 6 is consistent with ca. 50%-increase in DOC concentration in alkaline solutions in these experiments (Figure 4):

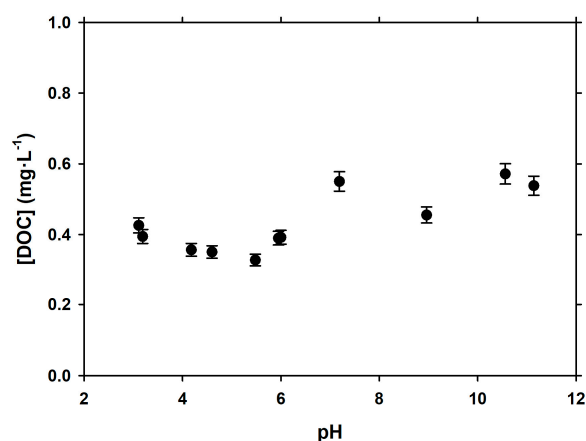


Figure 4. DOC concentration in experiments with 0.2 and 0.5 g_{wet}/L of EOMI diatoms after 60 min of exposure to 60 µg/L of *AuNPs* during 60 min. The error bars (s.d. of duplicates) are within the symbol size unless shown.

Another series of pH-edge experiments (Figure 5) were fitted in Sigmaplot using a Ligand binding equation for one site competition. This and the previously described result may have important consequences for understanding the *AuNPs* interaction with photosynthesizing diatoms

cells. It is possible that during the active phase of photosynthesis, during the day, when the pH in the pristine water layer surrounding the cells rises above 9, the diatoms will release *AuNPs* that were adsorbed at the cell surface during the dark phase of photosynthesis at night, at a lower pH than the surrounding medium. The pH 9.0 ± 0.5 is a threshold value where 50% of the initial *AuNPs* were desorbed. The model fit parameters with $R^2 = 0.91$ and Standard Error of Estimation 0.06 are listed in Table 2. No duplicates were run for these adsorption experiments; however, a large number of data points in adsorbed Au as a function of pH allowed an adequate estimation of relative experimental reproducibility.

Table 2. The model fit parameters of Equation (1) of *AuNPs* adsorption onto diatoms.

Parameter	Coefficient	Std. Error
<i>min</i>	11.69	0.189
<i>max</i>	12.77	0.0118
log <i>EC50</i>	9.81	0.142

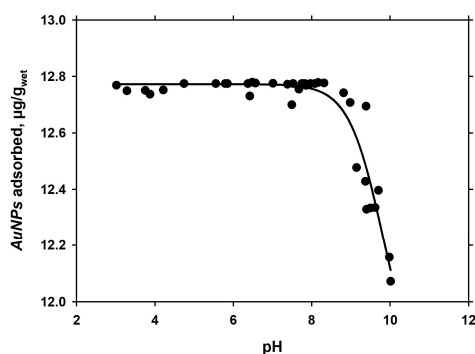


Figure 5. pH-dependence of *AuNPs* adsorption on the surface of diatoms EOMI (10 g_{wet}/L, 130 µg/L *AuNPs*, 2 h of reaction) and a one-site competition fit to the data.

3.3. Langmuirian Adsorption at Constant pH, as a Function of *AuNPs* in Solution

The stability of *AuNPs* was studied as a function of initial *AuNPs* concentration, for both 0.01 M NaCl and diatom cell supernatant. The contact time was 60 min.

The concentration of *AuNPs* increased linearly as a function of the concentration of *AuNPs* added to the solution. The loss of *AuNPs* was negligible for concentrations lower than 100 µg/L and it is more important for the higher concentrations (500 µg/L), as illustrated in Figure 6. Note that further experiments are necessary to discriminate the fraction that was precipitated during these stability tests.

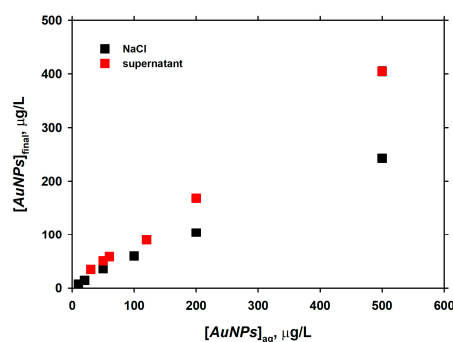


Figure 6. Stability of *AuNPs* in 0.01 M NaCl and cell supernatant solution for 0.2 and 0.5 g_{wet}/L of diatoms. The loss of *AuNPs* in blank experiments is 45% smaller in cell supernatant compared to the inert electrolyte (0.01 M NaCl). The error bars are within the symbol size unless shown.

The adsorption of *AuNPs* on diatoms was also studied for two initial biomass, 0.2 and 0.5 g_{wet}/L, as a function of *AuNPs* in solution at a constant pH of 6.0, as illustrated in Figure 7.

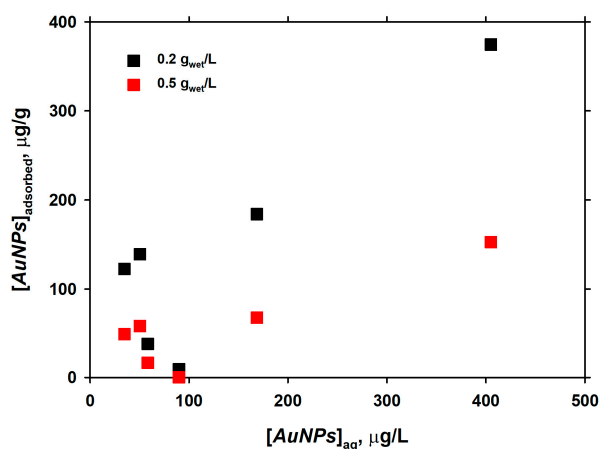


Figure 7. Adsorbed *AuNPs* as a function of aqueous *AuNPs* concentration in the presence of 0.2 and 0.5 g_{wet}/L of EOMI diatoms, at pH of 6. The error bars are within the symbol size unless shown.

Another set of experiments were performed to understand the adsorption of *AuNPs* onto diatoms after a 2 h exposure time and in the presence of 10 g_{wet} diatom/L in 5 mM NaCl and 5 mM NaHCO₃ (Figure 8). The adsorption of *AuNPs* also increased as a function of *AuNPs* in solution. The adsorption data were modelled using the Freundlich isotherm with the parameters listed in Table 3.

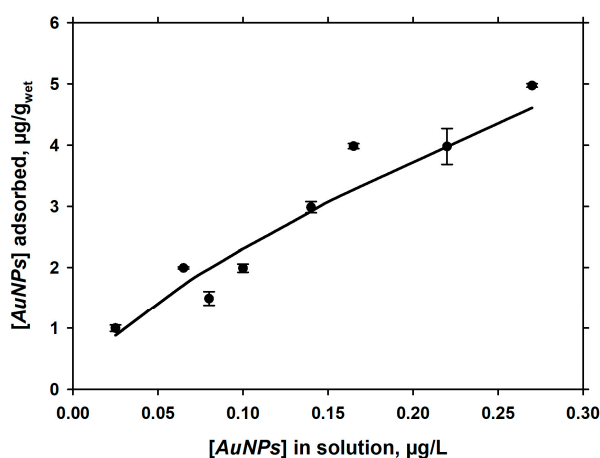


Figure 8. Low-range adsorption of *AuNPs* onto EOMI diatoms: concentration of adsorbed *AuNPs* at the surface of EOMI cells after 2 h mixing in 5 mM NaCl + 5 mM NaHCO₃ at pH = 8.50 ± 0.05. The solid line is a fit to the data using the Freundlich isotherm.

Table 3. Freundlich isotherm parameters for the adsorption of *AuNPs* on EOMI diatom as a function of *AuNPs* in solution. Dry biomass was always 10 g_{wet}/L.

Medium	pH	Contact Time (h)	log k_F	k_F (mol/L)	$1/n$	n (mol/L)
5 mM NaCl + 5 mM NaHCO ₃	8.56 ± 0.05	2	−0.459	0.347	0.696	1.436
10 mM NaCl	7.40 ± 0.06	1	0.621	4.177	1.115	0.897
	7.10 ± 0.06	24	0.035	1.085	1.014	0.986

The adsorption of *AuNPs* on EOMI surfaces was studied after 1 and 24 h of reaction at pH = 7.2 ± 0.2 in 0.01 M NaCl (Figure 9). It can be seen that the adsorption equilibrium was achieved within 1 h of

reaction, because there was no significant ($p < 0.05$) difference in the amount of adsorbed *AuNPs* after 1 and 24 h of reaction. The LPM fit of the adsorption data yielded $pK_m = 1.6$ and a binding site (BS) concentration of $14.5 \mu\text{mol}/g_{\text{wet}}$ for 1 h of reaction and $pK_1 = -2.2$ and $pK_2 = 1.0$ with BS values of 0.0037 and $6.5 \mu\text{mol}/g_{\text{wet}}$, respectively.

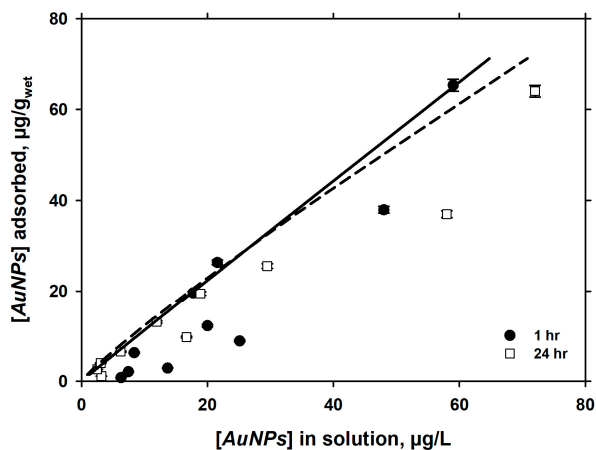


Figure 9. Adsorption of *AuNPs* on EOMI surfaces after 1 and 24 h of reaction at $\text{pH} = 7.2 \pm 0.2$ in 0.01 M NaCl . The solid lines represent a Freundlich isotherm fit to the data. The error bars are within the symbol size unless shown. They correspond to standard deviation of duplicates.

These experimental data were also fitted to the Freundlich isotherm and the parameters are shown in Table 3. The n value for all the experiments was close to one, implying a chemical adsorption process, except for the experiment in NaCl at a higher pH , where the n value was higher than 1 and where a combination of chemical and physical process could occur at the same time.

The adsorption capacities of EOMI cell surfaces with respect to *AuNPs* are fairly well (within 30%) comparable with that of *Navicula minima* with respect to Cd^{2+} , studied in previous works of our group [31].

3.4. Long-Term Interaction of *AuNPs* with Live Diatom Cells

Experiments of long-term interaction of diatoms with *AuNPs* aimed at comparing the adsorption + uptake of *AuNPs* by diatoms in the presence of light and in the darkness, over 20 to 50 days of exposure in the inert buffered media ($5 \text{ mM NaCl} + 5 \text{ mM NaHCO}_3$). At $100 \mu\text{g}/\text{L}$ of added *AuNPs* and a constant pH of 8.6, the major removal of *AuNPs* occurred over the first one to two days and it was more pronounced under light than in the darkness (Figure 10). We tentatively interpret this difference as due to two possible reasons. First, the pristine pH of the diatom cell surface during photosynthesis under light is higher than that of the surfaces in the darkness, and the adsorption of *AuNPs* on the cell surface strongly decreases above $\text{pH} 9$ (Figure 5). Note that, although the bulk solution is buffered at $\text{pH} 8.6$, the pristine pH of the photosynthesizing cell is typically 1 to 2 pH units higher, as is known from in-situ measurements with microelectrodes [39,46]. Second, the cells under light might be able to exudate various organic ligands, as is known in both freshwater and marine phytoplankton species [47–51].

Long-term experiments under light in the presence of 1 and $10 g_{\text{wet}}/\text{L}$ demonstrated an abrupt decrease in concentration of *AuNPs* over the first days of exposure, followed by a stable concentration of *AuNPs* (at $1 g_{\text{wet}}/\text{L}$ of EOMI) or an increase in $[AuNPs]$ by 40%–50% from the fourth to 55th day of exposure (Figure 11). We interpret this increase as due to exometabolites production and the removal of part of the adsorbed nanoparticles in the form of *AuNPs*-ligand complexes. The positive charge of *AuNPs* and negative charge of produced simple carboxylic acids or exopolysaccharides may cause such a desorption of *AuNPs* from the cell surface. Note that an alternative explanation, an efflux of

AuNPs from the cell to the surrounding medium, or a detoxification mechanism, triggered by high concentrations of *AuNPs*, is less likely: such an efflux was not visible in experiments with 1 g_{wet}/L EOMI at much higher concentrations of added *AuNPs* (Figure 10). As such, desorption via soluble exometabolites produced by a high amount of EOMI (10 g_{wet}/L) is the most likely cause of the aqueous *AuNPs* concentration increase over two months of exposure.

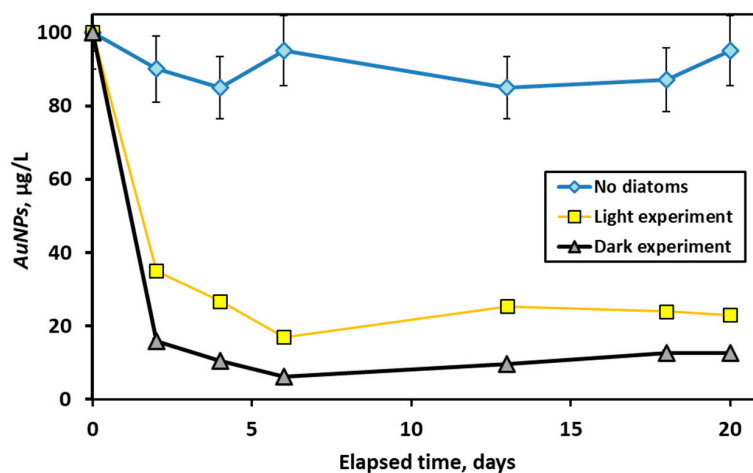


Figure 10. Concentration of *AuNPs* in 5 mM NaCl + 5 mM NaHCO₃ solution at pH = 8.6 ± 0.1 in the presence of 1 g_{wet}/L live EOMI diatoms under light (yellow squares) and in the darkness (grey triangles). The error bars (s.d. of duplicates) are within the symbol size unless shown.

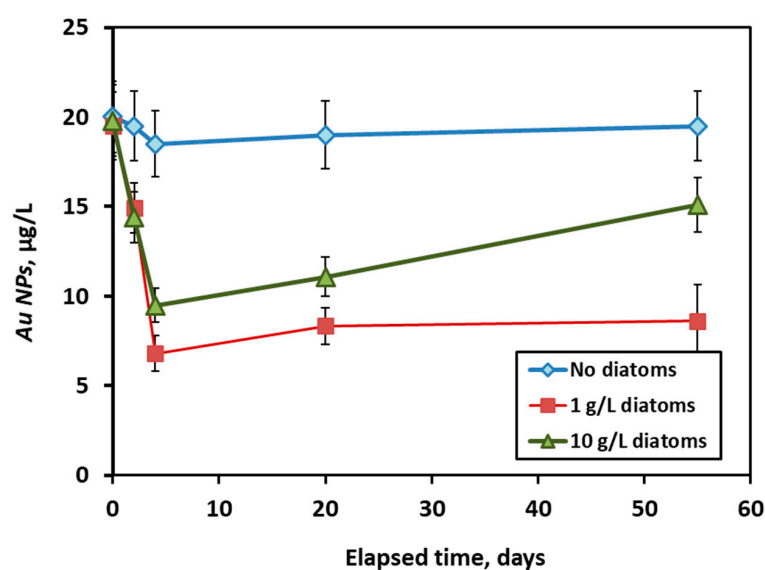


Figure 11. Concentration of *AuNPs* in 5 mM NaCl + 5 mM NaHCO₃ solution at pH = 8.7 ± 0.2 under light in the presence of 1 and 10 g_{wet}/L of live diatoms (green triangles and red squares, respectively). The error bars (standard deviation of duplicates) are shown by vertical lines.

4. Conclusions and Natural Applications

Results of our experiments demonstrated the efficiency of a thermodynamic and kinetic approach for characterizing the interaction between synthetic gold nanoparticles and freshwater periphytic diatoms EOMI. The dissolved organic matter (cell exometabolites) of diatom cells in the supernatant solution enhanced the stability of *AuNPs* in solution compared to that of the inert electrolyte. Positively charged *AuNPs* interacted with negatively charged diatom surfaces in a way similar to that of metal

cations, although some desorption of *AuNPs* from the cell surfaces at $\text{pH} > 9$ may be due to competition between soluble organic ligands produced by cell metabolism and cell surface moieties for *AuNPs*(+) complexation. Surface tertiary amine groups [52] or hybrid $\text{NH}_3^+/\text{COO}^-$ terminated surfaces as surrogates for charged ionisable groups of diatoms [53] are likely candidates for *AuNPs*-adsorbing moieties at the cell surfaces. The “Langmuirian” adsorption isotherm (at constant circumneutral pH) demonstrated adsorption capacities of EOMI cells that were similar to those of diatom *Navicula minima* with respect to divalent metal cations. We could not detect any significant long-term assimilation of *AuNPs* by diatom cells. Instead, the majority of nanoparticles were removed over the first hours to days of the surface adsorption reaction, followed by a slow release in the course of the following weeks.

Long-term (days to weeks) interaction of *AuNPs* with live diatom cells demonstrated the enhanced stability of *AuNPs* in the presence of photosynthesizing cells compared to cell-free solutions. This may be caused by (i) increasing pristine pH in the cell vicinity due to photosynthesis so that *AuNPs* are desorbed from the surface; and (ii) the production of cell exometabolites, which complexed positively-charged *AuNPs* and desorbed them from cell surface. An efflux of *AuNPs* as a detoxification mechanism seems to be subordinate to a desorption/complexation reaction.

In natural settings, cell photosynthesis should lead to a decrease in *AuNPs* adsorption and uptake by cells and thus can be considered as a mechanism of passive detoxification, driven by the exertion of organic ligands. Note that the stabilization of *AuNPs* by natural organic matter of a different molecular weight is well known from various laboratory experiments [43,44].

It is anticipated that a rigorous physico-chemical approach for the description of *AuNPs*-diatom interaction developed in the present study will help to establish a sound scientific basis for determining the quality status of water reservoirs and allow researchers to develop reliable predictive models of pollutants impact on aquatic ecosystems.

Acknowledgments: The work was supported by the Agence Nationale de la Recherche (ANR) in the CITTOXIC-Nano program (ANR-14-CE21-0001-01). Partial support from Russian National Scientific Fund (Grant No. 15-17-10009) is also acknowledged. Aridane G. González also thanks the postdoctoral program from the Universidad de Las Palmas de Gran Canaria.

Author Contributions: A.G.G. and O.S.P. conceived and designed the experiments; A.G.G., I.S.I., O.O. performed the experiments; A.G.G. and O.S.P. analyzed the data; S.M., M.B., and A.F.-M. contributed reagents/materials/analysis tools; O.S.P. and A.G.G. wrote the paper.

Conflicts of Interest: The authors declare no conflict of interest.

References

1. Chatterjee, A.; Priyam, A.; Bhattacharya, S.C.; Saha, A. pH dependent interaction of biofunctionalized CdS nanoparticles with nucleobases and nucleotides: A fluorimetric study. *J. Lumin.* **2007**, *126*, 764–770. [[CrossRef](#)]
2. Louis, C.; Pluchery, O. *Gold Nanoparticles for Physics, Chemistry and Biology*; World Scientific: Singapore, 2017; ISBN 1786341263.
3. Chen, H.-C.; Liu, Y.-C. Creating functional water by treating excited gold nanoparticles for the applications of green chemistry, energy and medicine: A review. *J. Ind. Eng. Chem.* **2017**, *60*, 9–18. [[CrossRef](#)]
4. Rothen-Rutishauser, B.M.; Schürch, S.; Haenni, B.; Kapp, N.; Gehr, P. Interaction of fine particles and nanoparticles with red blood cells visualized with advanced microscopic techniques. *Environ. Sci. Technol.* **2006**, *40*, 4353–4359. [[CrossRef](#)] [[PubMed](#)]
5. Russell, R.; Cresanti, R. *Environmental Health and Safety Research Needs for Engineered Nanoscale Materials*; Executive Office of the President Washington DC National Science and Technology Council: Washington, DC, USA, 2006.
6. Chang, M.R.; Lee, D.J.; Lai, J.Y. Nanoparticles in wastewater from a science-based industrial park-Coagulation using polyaluminum chloride. *J. Environ. Manag.* **2007**, *85*, 1009–1014. [[CrossRef](#)] [[PubMed](#)]
7. Charles, P.; Bizi, M.; Guiraud, P.; Labille, J.; Janex-Habibi, M.-L. NANOSEP: Removal of nanoparticles using optimized conventional processes. In Proceedings of the Water Quality Technology Conference and Exposition, Phoenix, AZ, USA, 13–17 November 2011; pp. 995–1004.

8. Bizi, M. Stability and flocculation of nanosilica by conventional organic polymer. *Nat. Sci.* **2012**, *4*, 372–385. [[CrossRef](#)]
9. Patwa, A.; Labille, J.; Bottero, J.-Y.; Thiéry, A.; Barthélémy, P. Decontamination of nanoparticles from aqueous samples using supramolecular gels. *Chem. Commun.* **2015**, *51*, 2547–2550. [[CrossRef](#)] [[PubMed](#)]
10. Auffan, M.; Rose, J.; Wiesner, M.R.; Bottero, J.Y. Chemical stability of metallic nanoparticles: A parameter controlling their potential cellular toxicity in vitro. *Environ. Pollut.* **2009**, *157*, 1127–1133. [[CrossRef](#)] [[PubMed](#)]
11. Connor, E.E.; Mwamuka, J.; Gole, A.; Murphy, C.J.; Wyatt, M.D. Gold nanoparticles are taken up by human cells but do not cause acute cytotoxicity. *Small* **2005**, *1*, 325–327. [[CrossRef](#)] [[PubMed](#)]
12. Shukla, R.; Bansal, V.; Chaudhary, M.; Basu, A.; Bhonde, R.R.; Sastry, M. Biocompatibility of gold nanoparticles and their endocytotic fate inside the cellular compartment: A microscopic overview. *Langmuir* **2005**, *21*, 10644–10654. [[CrossRef](#)] [[PubMed](#)]
13. Tedesco, S.; Doyle, H.; Blasco, J.; Redmond, G.; Sheehan, D. Exposure of the blue mussel, *Mytilus edulis*, to gold nanoparticles and the pro-oxidant menadione. *Comp. Biochem. Physiol. C Toxicol. Pharmacol.* **2010**, *151*, 167–174. [[CrossRef](#)] [[PubMed](#)]
14. Baudrimont, M.; Andrei, J.; Mornet, S.; Gonzalez, P.; Mesmer-Dudons, N.; Gourves, P.Y.; Jaffal, A.; Dedourge-Geffard, O.; Geffard, A.; Geffard, O.; et al. Trophic transfer and effects of gold nanoparticles (AuNPs) in *Gammarus fossarum* from contaminated periphytic biofilm. *Environ. Sci. Pollut. Res.* **2017**, 1–11. [[CrossRef](#)] [[PubMed](#)]
15. Cho, W.S.; Cho, M.; Jeong, J.; Choi, M.; Cho, H.Y.; Han, B.S.; Kim, S.H.; Kim, H.O.; Lim, Y.T.; Chung, B.H.; et al. Acute toxicity and pharmacokinetics of 13 nm-sized PEG-coated gold nanoparticles. *Toxicol. Appl. Pharmacol.* **2009**, *236*, 16–24. [[CrossRef](#)] [[PubMed](#)]
16. Farkas, J.; Christian, P.; Urrea, J.A.G.; Roos, N.; Hassellöv, M.; Tollefsen, K.E.; Thomas, K.V. Effects of silver and gold nanoparticles on rainbow trout (*Oncorhynchus mykiss*) hepatocytes. *Aquat. Toxicol.* **2010**, *96*, 44–52. [[CrossRef](#)] [[PubMed](#)]
17. Tedesco, S.; Doyle, H.; Redmond, G.; Sheehan, D. Gold nanoparticles and oxidative stress in *Mytilus edulis*. *Mar. Environ. Res.* **2008**, *66*, 131–133. [[CrossRef](#)] [[PubMed](#)]
18. Renault, S.; Baudrimont, M.; Mesmer-Dudons, N.; Gonzalez, P.; Mornet, S.; Brisson, A. Impacts of gold nanoparticle exposure on two freshwater species: A phytoplanktonic alga (*Scenedesmus subspicatus*) and a benthic bivalve (*Corbicula fluminea*). *Gold Bull.* **2008**, *41*, 116–126. [[CrossRef](#)]
19. Lapresta-Fernández, A.; Fernández, A.; Blasco, J. Nanoecotoxicity effects of engineered silver and gold nanoparticles in aquatic organisms. *TrAC Trends Anal. Chem.* **2012**, *32*, 40–59. [[CrossRef](#)]
20. Mahaye, N.; Thwala, M.; Cowan, D.A.; Musee, N. Genotoxicity of metal based engineered nanoparticles in aquatic organisms: A review. *Mutat. Res. Rev. Mutat. Res.* **2017**, *773*, 134–160. [[CrossRef](#)] [[PubMed](#)]
21. Fein, J.B.; Daughney, C.J.; Yee, N.; Davis, T.A. A chemical equilibrium model of metal adsorption onto bacterial surfaces. *Geochim. Cosmochim. Acta* **1997**, *61*, 3319–3328. [[CrossRef](#)]
22. Boyanov, M.I.; Kelly, S.D.; Kemner, K.M.; Bunker, B.A.; Fein, J.B.; Fowle, D.A. Adsorption of cadmium to *Bacillus subtilis* bacterial cell walls: A pH-dependent X-ray absorption fine structure spectroscopy study. *Geochim. Cosmochim. Acta* **2003**, *67*, 3299–3311. [[CrossRef](#)]
23. Burnett, P.G.G.; Daughney, C.J.; Peak, D. Cd adsorption onto *Anoxybacillus flavithermus*: Surface complexation modeling and spectroscopic investigations. *Geochim. Cosmochim. Acta* **2006**, *70*, 5253–5269. [[CrossRef](#)]
24. Guiné, V.; Spadini, L.; Sarret, G.; Muris, M.; Delolme, C.; Gaudet, J.-P.; Martins, J.M.F. Zinc sorption to three gram-negative bacteria: Combined titration, modeling, and EXAFS study. *Environ. Sci. Technol.* **2006**, *40*, 1806–1813. [[CrossRef](#)] [[PubMed](#)]
25. Fein, J.B.; Martin, A.M.; Wightman, P.G. Metal adsorption onto bacterial surfaces: Development of a predictive approach. *Geochim. Cosmochim. Acta* **2001**, *65*, 4267–4273. [[CrossRef](#)]
26. Martinez, R.E.; Ferris, F.G.G. Chemical equilibrium modeling techniques for the analysis of high-resolution bacterial metal sorption data. *J. Colloid Interface Sci.* **2001**, *243*, 73–80. [[CrossRef](#)]
27. Martinez, R.E.; Pedersen, K.; Ferris, F.G. Cadmium complexation by bacteriogenic iron oxides from a subterranean environment. *J. Colloid Interface Sci.* **2004**, *275*, 82–89. [[CrossRef](#)] [[PubMed](#)]
28. Borrok, D.M.; Fein, J.B.; Kulpa, C.F.J. Cd and Proton adsorption onto bacterial grown from industrial wastes and contaminated geologic settings. *Environ. Sci. Technol.* **2004**, *38*, 5656–5664. [[CrossRef](#)] [[PubMed](#)]

29. Borrok, D.; Turner, B.F.; Fein, J.B. A universal surface complexation framework for modeling proton binding onto bacterial surfaces in geologic settings. *Am. J. Sci.* **2005**, *305*, 826–853. [[CrossRef](#)]
30. Gélabert, A.; Pokrovsky, O.S.; Viers, J.; Schott, J.; Boudou, A.; Feurtet-Mazel, A. Interaction between zinc and freshwater and marine diatom species: Surface complexation and Zn isotope fractionation. *Geochim. Cosmochim. Acta* **2006**, *70*, 839–857. [[CrossRef](#)]
31. Gélabert, A.; Pokrovsky, O.S.; Schott, J.; Boudou, A.; Feurtet-Mazel, A. Cadmium and lead interaction with diatom surfaces: A combined thermodynamic and kinetic approach. *Geochim. Cosmochim. Acta* **2007**, *71*, 3698–3716. [[CrossRef](#)]
32. González, A.G.; Pokrovsky, O.S.; Jiménez-Villacorta, F.; Shirokova, L.S.; Santana-Casiano, J.M.; González-Dávila, M.; Emnova, E.E. Iron adsorption onto soil and aquatic bacteria: XAS structural study. *Chem. Geol.* **2014**, *372*, 32–45. [[CrossRef](#)]
33. González, A.G.; Jimenez-Villacorta, F.; Beike, A.K.; Reski, R.; Adamo, P.; Pokrovsky, O.S. Chemical and structural characterization of copper adsorbed on mosses (Bryophyta). *J. Hazard. Mater.* **2016**, *308*, 343–354. [[CrossRef](#)] [[PubMed](#)]
34. Gélabert, A.; Pokrovsky, O.S.; Schott, J.; Boudou, A.; Feurtet-Mazel, A.; Mielczarski, J.; Mielczarsky, E.; Mesmer-Dudons, N.; Spalla, O. Study of diatoms/aqueous solution interface. I. Acid-base equilibria, surface charge and spectroscopic observation of two freshwater periphytic and two marine planktonic diatoms. *Geochim. Cosmochim. Acta* **2004**, *68*, 4039–4058. [[CrossRef](#)]
35. Kim Tiam, S.; Feurtet-Mazel, A.; Delmas, F.; Mazzella, N.; Morin, S.; Daffe, G.; Gonzalez, P. Development of q-PCR approaches to assess water quality: Effects of cadmium on gene expression of the diatom *Eolimna minima*. *Water Res.* **2012**, *46*, 934–942. [[CrossRef](#)] [[PubMed](#)]
36. Moisset, S.; Tiam, S.K.; Feurtet-Mazel, A.; Morin, S.; Delmas, F.; Mazzella, N.; Gonzalez, P. Genetic and physiological responses of three freshwater diatoms to realistic diuron exposures. *Environ. Sci. Pollut. Res.* **2015**, *22*, 4046–4055. [[CrossRef](#)] [[PubMed](#)]
37. Feurtet-Mazel, A.; Mornet, S.; Charron, L.; Mesmer-Dudons, N.; Maury-Brachet, R.; Baudrimont, M. Biosynthesis of gold nanoparticles by the living freshwater diatom *Eolimna minima*, a species developed in river biofilms. *Environ. Sci. Pollut. Res.* **2016**, *23*, 4334–4339. [[CrossRef](#)] [[PubMed](#)]
38. Gold, C.; Feurtet-Mazel, A.; Coste, M.; Boudou, A. Impacts of Cd and Zn on the development of periphytic diatom communities in artificial streams located along a river pollution gradient. *Arch. Environ. Contam. Toxicol.* **2003**, *44*, 189–197. [[CrossRef](#)] [[PubMed](#)]
39. Pokrovsky, O.S.; Martinez, R.E.; Golubev, S.V.; Kompantseva, E.I.; Shirokova, L.S. Adsorption of metals and protons on *Gloeocapsa* sp. cyanobacteria: A surface speciation approach. *Appl. Geochem.* **2008**, *23*, 2574–2588. [[CrossRef](#)]
40. Pokrovsky, O.S.; Martinez, R.E.; Kompantseva, E.I.; Shirokova, L.S. Surface complexation of the phototrophic anoxygenic non-sulfur bacterium *Rhodospseudomonas palustris*. *Chem. Geol.* **2014**, *383*, 51–62. [[CrossRef](#)]
41. González, A.G.; Shirokova, L.S.; Pokrovsky, O.S.; Emnova, E.E.; Martínez, R.E.; Santana-Casiano, J.M.; González-Dávila, M.; Pokrovski, G.S. Adsorption of copper on *Pseudomonas aureofaciens*: Protective role of surface exopolysaccharides. *J. Colloid Interface Sci.* **2010**, *350*, 305–314. [[CrossRef](#)] [[PubMed](#)]
42. Pokrovsky, O.S.; Feurtet-Mazel, A.; Martinez, R.E.; Morin, S.; Baudrimont, M.; Duong, T.; Coste, M. Experimental study of cadmium interaction with periphytic biofilms. *Appl. Geochem.* **2010**, *25*, 418–427. [[CrossRef](#)]
43. Stankus, D.P.; Lohse, S.E.; Hutchison, J.E.; Nason, J.A. Interactions between natural organic matter and gold nanoparticles stabilized with different organic capping agents. *Environ. Sci. Technol.* **2011**, *45*, 3238–3244. [[CrossRef](#)] [[PubMed](#)]
44. Louie, S.M.; Spielman-Sun, E.R.; Small, M.J.; Tilton, R.D.; Lowry, G.V. Correlation of the physicochemical properties of natural organic matter samples from different sources to their effects on gold nanoparticle aggregation in monovalent electrolyte. *Environ. Sci. Technol.* **2015**, *49*, 2188–2198. [[CrossRef](#)] [[PubMed](#)]
45. Yu, Q.; Fein, J.B. Sulfhydryl binding sites within bacterial extracellular polymeric substances. *Environ. Sci. Technol.* **2016**, *50*, 5498–5505. [[CrossRef](#)] [[PubMed](#)]
46. Bundelava, I.A.; Shirokova, L.S.; Pokrovsky, O.S.; Bénézech, P.; Ménez, B.; Gérard, E.; Balor, S. Experimental modeling of calcium carbonate precipitation by cyanobacterium *Gloeocapsa* sp. *Chem. Geol.* **2014**, *374–375*, 44–60. [[CrossRef](#)]

47. Rico, M.; López, A.; Santana-Casiano, J.M.; González, A.G.; González-Dávila, M. Variability of the phenolic profile in the diatom *Phaeodactylum tricorutum* growing under copper and iron stress. *Limnol. Oceanogr.* **2013**, *51*, 144–152. [[CrossRef](#)]
48. González, A.G.; Santana-Casiano, J.M.; González-Dávila, M.; Pérez-Almeida, N.; Suárez de Tangil, M. Effect of *Dunaliella tertiolecta* organic exudates on the Fe(II) oxidation kinetics in seawater. *Environ. Sci. Technol.* **2014**, *48*, 7933–7941. [[CrossRef](#)] [[PubMed](#)]
49. González, A.G.; Santana-Casiano, J.M.; González-Dávila, M.; Perez, N. Effect of organic exudates of *Phaeodactylum tricorutum* on the Fe(II) oxidation rate constant. *Cienc. Mar.* **2012**, *38*, 245–261. [[CrossRef](#)]
50. Santana-Casiano, J.M.; González-Dávila, M.; González, A.G.; Rico, M.; Lopez, A.; Martel, A. Characterization of phenolic exudates from *Phaeodactylum tricorutum* and their effects on the chemistry of Fe(II)-Fe(III). *Mar. Chem.* **2014**, *158*, 10–16. [[CrossRef](#)]
51. González, A.G.; Fernández-Rojo, L.; Leflaive, J.; Pokrovsky, O.S.; Rols, J.L. Response of three biofilm-forming benthic microorganisms to Ag nanoparticles and Ag⁺: The diatom *Nitzschia palea*, the green alga *Uronema confervicolum* and the cyanobacteria *Leptolyngbya* sp. *Environ. Sci. Pollut. Res.* **2016**, *23*, 22136–22150. [[CrossRef](#)] [[PubMed](#)]
52. Pohnert, G. Biomineralization in diatoms mediated through peptide- and polyamine-assisted condensation of silica. *Angew. Chem. Int. Ed.* **2002**, *41*, 3167–3169. [[CrossRef](#)]
53. Wallace, A.F.; DeYoreo, J.J.; Dove, P.M. Kinetics of silica nucleation on carboxyl- and amine-terminated surfaces: Insights for biomineralization. *J. Am. Chem. Soc.* **2009**, *131*, 5244–5250. [[CrossRef](#)] [[PubMed](#)]



© 2018 by the authors. Licensee MDPI, Basel, Switzerland. This article is an open access article distributed under the terms and conditions of the Creative Commons Attribution (CC BY) license (<http://creativecommons.org/licenses/by/4.0/>).